

Gradient-flowed thermal correlators: How much flow is too much?

Alexander M. Eller* and Guy D. Moore†

*Institut für Kernphysik, Technische Universität Darmstadt, Schlossgartenstraße 2,
D-64289 Darmstadt, Germany*

(Received 16 May 2018; published 11 June 2018)

Gradient flow has been proposed in the lattice community as a tool to reduce the sensitivity of operator correlation functions to noisy UV fluctuations. We test perturbatively under what conditions doing so may contaminate the results. To do so, we compute gradient-flowed electric field two-point correlators and stress-tensor one- and two-point correlators at finite temperature in QCD. Gradient flow has almost no influence on the value of correlators until a (temperature- and separation-dependent) level of flow is reached, after which the correlator is rapidly compromised. We provide a prescription for how much flow is “safe.”

DOI: [10.1103/PhysRevD.97.114507](https://doi.org/10.1103/PhysRevD.97.114507)**I. INTRODUCTION**

Gradient flow [1–12] is a nonperturbative and gauge-invariant method in quantum field theory for defining not-quite-local operators with greatly improved insensitivity to ultraviolet fluctuations. Gradient flow is defined by introducing a procedure which, configuration by configuration within the Euclidean path integral, applies “heat equation” evolution to the fields, before constructing operators out of them. Roughly speaking, one can think of this as replacing the fields in an operator with those averaged over a Gaussian envelope. However, by using a nonlinear and gauge-invariant version of the heat equation, the procedure maintains gauge invariance. One can make a rigorous connection between operators under gradient flow and renormalized operators, and all perturbation theory tools needed to study gradient-flowed operators have been developed [5].

The main applications of gradient flow have been within lattice quantum field theory. The value of the F^2 operator ($F^{\mu\nu}$ the field strength) as a function of scale can be used to “read off” the scale-dependent coupling constant and therefore to perform scale setting [9]. This can also be used to extract the $\overline{\text{MS}}$ coupling, where the value of the F^2 operator under flow is now known to next-to-next-to-leading order [13]. Gradient flow is also now widely used to remove UV fluctuations which contaminate the determination of topology on the lattice [14–20]. This is similar to older “smearing” methods [21], with the difference that the gradient-flow approach is on more solid field theoretical foundations.

Gradient flow has also seen its first applications to the study of thermodynamical properties of finite-temperature systems. The energy density and pressure of SU(3) gauge theory were calculated directly on the lattice using gradient flow [22]. This was recently expanded to the energy-momentum tensor in order to determine the equation of state for SU(3) gauge theory [23]. The great advantage of gradient flow in this context is that, by reducing sensitivity to ultraviolet fluctuations, it can dramatically reduce statistical fluctuations in evaluating thermal operator expectation values and correlation functions. For instance, consider the determination of thermodynamical information. One could evaluate the energy density at temperature by evaluating the difference $\langle T^{00} \rangle_\beta - \langle T^{00} \rangle_{\text{vac}}$, the thermal-to-vacuum difference in the 00 component of the stress tensor. The configuration-by-configuration squared fluctuations in this quantity are set by the two-point function $\lim_{x \rightarrow 0} \langle T^{00}(x) T^{00}(0) \rangle$. Based on operator dimension, we see that this quantity diverges at small x as x^{-8} . Of course on the lattice this divergence is cut off by the lattice spacing and is $\mathcal{O}(a^{-8})$. This squared fluctuation must be compared to β^{-8} , the square of the size of the energy density difference; the number of spacetime points times configurations must compensate this large ratio to obtain a statistically significant measurement. On the other hand, under gradient flow to a depth τ_F , we expect the overlapping two-point function to be $\mathcal{O}(\tau_F^{-4})$ (τ_F has dimensions of length², not length). Therefore the UV fluctuations which inhibit a statistically significant evaluation are ameliorated and the number of configurations we must evaluate to obtain good statistics is reduced by a factor¹ of $(a^2/\tau_F)^2$.

*meller@theorie.ikp.physik.tu-darmstadt.de
†guy.moore@physik.tu-darmstadt.de

Published by the American Physical Society under the terms of the Creative Commons Attribution 4.0 International license. Further distribution of this work must maintain attribution to the author(s) and the published article's title, journal citation, and DOI. Funded by SCOAP³.

¹The factor is $(a^2/\tau_F)^2$ and not $(a^2/\tau_F)^4$ because there is only one independent measurement per τ_F^2 of volume, rather than every a^4 of volume.

A little gradient flow is certainly a good thing, improving statistics, fixing some operator renormalization issues [3], and making the lattice more continuumlike. However, too much gradient flow is definitely bad, as eventually we erase the fluctuations responsible for the physics we want to study. In particular, we want to know, for the study of thermal one-operator and multioperator correlators, exactly how much gradient flow one may apply before one changes the physics of interest. Previously several authors have performed empirical investigations to study the limitations to the use of gradient flow on the lattice in the context of nonlocal objects such as Wilson loops, Polyakov loops, and Wilson-line separated fermions [24–31]. The goal of this work is to go beyond empirical arguments and give an analytical study of the flow time dependence of correlation functions, specializing to finite temperature.

In this note we will study this problem perturbatively. To our knowledge this is the first perturbative study of thermal correlation functions, and of correlators of spacetime-separated operators, under gradient flow. Therefore we will content ourselves for the moment with a leading-order perturbative evaluation, which will already provide lessons on how much flow we may and may not use. In the future we want to extend this investigation beyond leading order, to see whether interactions significantly impact its findings.

Here we will consider three types of correlation functions. First and simplest, we consider the stress-tensor one-point function at finite temperature. As discussed above, this can be used to measure rather directly the energy density as a function of temperature (if the operator renormalization issues can be resolved; so far the renormalization of a gradient-flowed stress tensor has only been studied perturbatively [5,10], while a nonperturbative treatment is probably necessary). Second, we will consider the correlator of two electric field operators, embedded along a Polyakov line:

$$G^{\text{EE}}(\tau) = \frac{\langle \text{ReTr}U(\beta, 0; \tau, 0)E_i(\tau, 0)U(\tau, 0; 0, 0)E_i(0, 0) \rangle}{\langle \text{ReTr}U(\beta, 0; 0, 0) \rangle} \quad (1.1)$$

where $U(t_1, x_1; t_2, x_2)$ is a straight Wilson line from point (t_1, x_1) to point (t_2, x_2) and E_i is the electric field. This operator was introduced in [32], whose authors showed that its analytical continuation to Minkowski frequency determines the (momentum-space and coordinate-space) diffusion of a heavy quark, $m_q \gg T$ in a thermal bath. Recently there has been a vigorous effort to measure this correlation function on the lattice [33], but so far only quenched results are available and the issue of the E -field renormalization has not been resolved. Gradient flow would fix the renormalization issue and will hopefully improve statistical power such that the correlation function can be reliably measured at the nonperturbative level. Finally, we will consider the correlation function of two stress tensors at vanishing spatial

momentum (equivalently, integrated over spatial separation) as a function of the Euclidean time separation τ . For those $T^{\mu\nu}$ components which couple to hydrodynamical modes, such as $T^{00}T^{00}$ and $T^{0i}T^{0i}$, the correlator should be τ independent and should reproduce thermodynamical information (the heat conductivity and enthalpy density respectively). For the $\ell = 2$ space component, e.g., $T^{xy}T^{xy}$, the analytical continuation of the correlator holds information about the shear viscosity [34–37].

In the next section we will develop perturbative tools for gradient flow at finite temperature in coordinate space, which turns out to be the most convenient for the problems we study here. Next, Sec. III contains the specific details of the leading-order calculations of each correlator mentioned above. In every case we find that there is a (τ -dependent) range of flow times τ_F for which the correlator feels exponentially suppressed corrections; but for more flow it quickly goes wrong. We end with a discussion which presents our recommendations for the amount of flow which can be applied “safely,” given our lowest-order perturbative results.

II. GRADIENT FLOW AT TEMPERATURE IN COORDINATE SPACE

We write the unflowed gauge field as $A_\mu^a(x)$ and will generally suppress the color index a . The flowed gauge field $B_\mu(x, \tau_F)$ is defined at non-negative flow time τ_F through the $\tau_F = 0$ boundary condition

$$B_\mu(x, \tau_F)|_{\tau_F=0} = A_\mu(x) \quad (2.1)$$

and the flow equation

$$\frac{\partial B_\mu(x, \tau_F)}{\partial \tau_F} = D_\nu G_{\nu\mu}(x, \tau_F) + \alpha_0 D_\mu \partial_\nu B_\nu(x, \tau_F), \quad (2.2)$$

where $G_{\nu\mu}(x, \tau_F)$ is the field strength tensor written using $B_\mu(x, \tau_F)$ rather than $A_\mu(x)$. The second term in the flow equation constitutes a τ_F -dependent gauge choice, which is convenient to make in the context of perturbative calculations [3]. Choosing $\alpha_0 = 1$ and working to linearized order, the flow equation simplifies to

$$\frac{\partial B_\mu(x, \tau_F)}{\partial \tau_F} = \partial_\nu \partial_\nu B_\mu(x, \tau_F), \quad (2.3)$$

which is the heat equation.

In vacuum, the Feynman-gauge momentum-space propagator after flow is

$$\begin{aligned} G_E^{BB}(p, \tau_{F_1}, \tau_{F_2}) &= \int d^4x e^{ip_\mu x^\mu} \langle B_\mu(x, \tau_{F_1}) B_\nu(0, \tau_{F_2}) \rangle \\ &= g^2 \delta_{\mu\nu} \frac{e^{-(\tau_{F_1} + \tau_{F_2})p^2}}{p^2} \end{aligned} \quad (2.4)$$

and Fourier transforming leads to the zero temperature flowed propagator in coordinate space

$$G_E^{BB}(x, \tau_{F_1}, \tau_{F_2}) = \frac{g^2 \delta_{\mu\nu}}{4\pi^2 x^2} \left(1 - e^{-\frac{x^2}{4(\tau_{F_1} + \tau_{F_2})}}\right). \quad (2.5)$$

This result was found by Lüscher in [3]. But we could have reached this result faster by noting that the coordinate-space propagator before flow is the solution to the Poisson equation $-\partial_\mu^2 G_E^{AA}(x) = g^2 \delta^4(x)$, which is $G_E^{AA}(x) = g^2/(4\pi^2 x^2)$. At tree level and in Feynman gauge, flow is the application of the heat equation to this propagator, which is the same as convolving it with a Gaussian envelope,

$$\begin{aligned} G_E^{BB}(x, \tau_{F_1}, \tau_{F_2}) &= \int d^4 y \frac{g^2}{4\pi^2 y^2} e^{-\frac{(x-y)^2}{4(\tau_{F_1} + \tau_{F_2})}} \\ &= \frac{g^2}{4\pi^2 x^2} \left(1 - e^{-\frac{x^2}{4(\tau_{F_1} + \tau_{F_2})}}\right). \end{aligned} \quad (2.6)$$

Alternatively, one may take the right-hand expression as an ansatz and verify that it satisfies the $\tau_F = 0$ boundary conditions and the heat equation.

To introduce finite temperature, we restrict the Euclidean time to lie in $x^0 \in [0, \beta]$ with periodic boundary conditions. The fast way to find the coordinate-space propagator is to note that the Poisson equation is now solved using the method of images,

$$G_{E,\beta}^{AA}(x^0, \vec{x}) = \sum_{n \in \mathbb{Z}} \frac{g^2}{4\pi^2 x_n^2}, \quad x_n^\mu \equiv (x^0 + n\beta, \vec{x}), \quad (2.7)$$

and that flow again corresponds to evolving this propagator under the heat equation or convolving with a Gaussian:

$$G_{E,\beta}^{BB}(x, \tau_{F_1}, \tau_{F_2}) = \sum_{n=-\infty}^{\infty} \frac{g^2 \delta_{\mu\nu}}{4\pi^2 x_n^2} \left(1 - e^{-\frac{x_n^2}{4(\tau_{F_1} + \tau_{F_2})}}\right). \quad (2.8)$$

We could also arrive at this result the ‘‘hard way’’ by Fourier transforming the finite-temperature, flowed momentum-space propagator

$$G_{E,\beta}^{BB}(x, \tau_{F_1}, \tau_{F_2}) = T \sum_{p^0=2\pi mT}^{m \in \mathbb{Z}} \int \frac{d^3 p}{(2\pi)^3} e^{ip \cdot x} \times \frac{g^2 e^{-p^2(\tau_{F_1} + \tau_{F_2})}}{p^2} \quad (2.9)$$

by use of Poisson’s summation formula [38]

$$T \sum_{p^0=2\pi mT}^{m \in \mathbb{Z}} = \sum_{n \in \mathbb{Z}} \int_{-\infty}^{\infty} \frac{dp^0}{2\pi} e^{ip^0 \beta n} \quad (2.10)$$

to rewrite the summation over p^0 as a sum over coordinate-space copies—essentially, the same images as above.

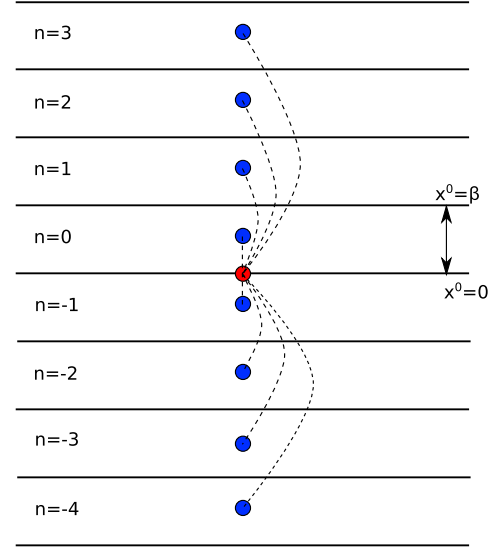


FIG. 1. The images and correlation of the finite-temperature gauge-field propagator. The colored circles represent the gauge fields, the horizontal lines the periodic boundaries in the time plane, and the dashed lines the correlations between one field and the images of the other.

At this point each $\int dp^0$ term represents a vacuum contribution with a different x^0 position, shifted into one of the image copies. This leads rather directly back to Eq. (2.8). In the following we will only work at finite temperature so we will suppress the subscript β .

When we take correlation functions, we will have to include a sum over images for *each* propagator which appears. We present an illustration of this procedure in Fig. 1.

III. CALCULATIONS

We will now use the coordinate-space propagator to compute the desired correlation functions. While the last section has introduced propagators between fields with different amounts of flow, here we will only consider correlators where all operators are evaluated after the same amount of flow τ_F ; so the previous formulas should be modified by writing $\tau_{F_1} = \tau_{F_2} = \tau_F$.

A. Energy-Momentum Tensor One-Point Function

The tree-level energy-momentum tensor in Yang-Mills theory is²

$$\begin{aligned} T_{\mu\nu}^B(x, \tau_F) &= \frac{1}{g^2} \left[(G_{\mu\sigma}^a G_{\nu\sigma}^a)(x, \tau_F) - \frac{1}{4} \delta_{\mu\nu} (G_{\omega\sigma}^a G_{\omega\sigma}^a)(x, \tau_F) \right], \\ G_{\mu\nu}(x, \tau_F) &= \partial_\mu^x B_\nu(x, \tau_F) - \partial_\nu^x B_\mu(x, \tau_F). \end{aligned} \quad (3.1)$$

²At the loop level we would need to include the trace anomaly.

We evaluate the correlator of two field strengths by splitting the field strengths to reside at points x, y ; write

$$\langle B_\mu(x, \tau_F) B_\nu(y, \tau_F) \rangle = G_E^{BB}(x - y, \tau_F) \quad (3.2)$$

which we found in Eq. (2.8); take derivatives; and then set $x = y$. Introducing a dimensionless rescaled flow time $\tilde{\tau}_F \equiv 8\tau_F/\beta^2$, we evaluate the two field strength correlators which we need,

$$\langle G_{0\sigma}^a G_{0\sigma}^a \rangle = \frac{3g^2 d_A}{\pi^2 \beta^4} \sum_{n \in \mathbb{Z}} \left[e^{-\frac{n^2}{\tilde{\tau}_F}} \cdot \left(\frac{1}{\tilde{\tau}_F^2} + \frac{1}{\tilde{\tau}_F} \frac{1}{n^2} + \frac{1}{n^4} \right) - \frac{1}{n^4} \right], \quad (3.3)$$

$$\langle G_{i\sigma}^a G_{i\sigma}^a \rangle = \frac{3g^2 d_A}{\pi^2 \beta^4} \sum_{n \in \mathbb{Z}} \left[e^{-\frac{n^2}{\tilde{\tau}_F}} \cdot \left(\frac{1}{\tilde{\tau}_F^2} - \frac{1}{\tilde{\tau}_F} \frac{1}{n^2} - \frac{1}{n^4} \right) + \frac{1}{n^4} \right], \quad (3.4)$$

where each n^2 arises as x_n^2/β^2 . Then we combine them to find a closed expression for the stress-tensor one-point function after flow,

$$\langle T_{00} \rangle = -\langle T_{ii} \rangle = \frac{3d_A}{\pi^2 \beta^4} \sum_{n \in \mathbb{Z}} \left[e^{-\frac{n^2}{\tilde{\tau}_F}} \cdot \left(\frac{1}{2\tilde{\tau}_F^2} + \frac{1}{\tilde{\tau}_F} \frac{1}{n^2} + \frac{1}{n^4} \right) - \frac{1}{n^4} \right]. \quad (3.5)$$

Here $d_A = N_c^2 - 1 = 8$ is the dimension of the group, which counts gluon colors. The sum over n is a sum over images; the vacuum result is the $n = 0$ term, which is defined as the $n \rightarrow 0$ limit and which actually vanishes. In the $\tau_F \rightarrow 0$ limit the exponential terms vanish and we have only the $1/n^4$ term, confirming as expected that

$$\langle T_{00} \rangle = -\frac{3d_A}{\pi^2 \beta^4} \sum_{n \neq 0} \frac{1}{n^4} = -\frac{6d_A}{\pi^2 \beta^4} \zeta(4), \quad (3.6)$$

the standard Stefan-Boltzmann result.

In the opposite limit, $\tilde{\tau}_F \gg 1$, many terms contribute to the sum and we may approximate it with an integral, giving rise to

$$\begin{aligned} \langle T_{00} \rangle_\beta \xrightarrow{\tilde{\tau}_F \gg 1} & \frac{3d_A}{\pi^2 \beta^4} \frac{1}{\tilde{\tau}_F^{3/2}} \int_{-\infty}^{\infty} du \frac{1}{u^4} \left[-1 + \left(1 + u^2 + \frac{u^4}{2} \right) e^{-u^2} \right] \\ & = -\frac{3d_A}{\pi^2 \beta^4} \frac{1}{\tilde{\tau}_F^{3/2}} \frac{\sqrt{\pi}}{6} = -\frac{d_A}{32\sqrt{2}\pi^{3/2}\tilde{\tau}_F^{3/2}\beta}. \end{aligned} \quad (3.7)$$

This result corresponds to the contribution arising from the zero Matsubara frequency, as all other Matsubara frequencies are damped away by the flow.

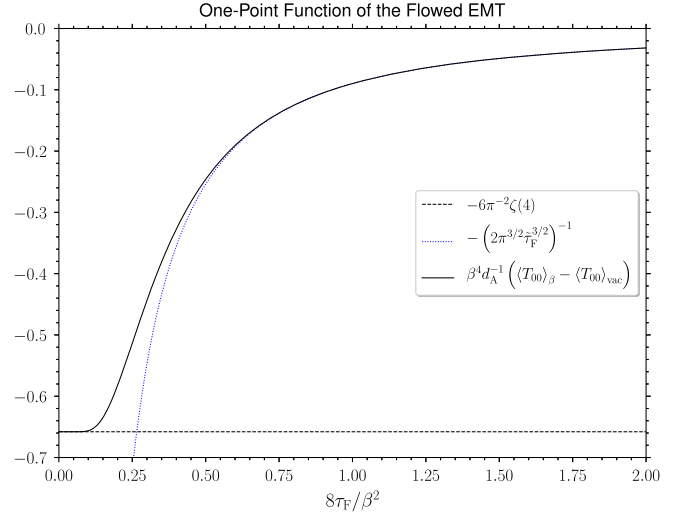


FIG. 2. Plot of the one-point function of the energy-momentum tensor as a function of the applied gradient flow, together with its asymptotic small τ_F and large τ_F behavior.

For finite $\tilde{\tau}_F$ we evaluate the sum numerically and display the result in Fig. 2. The plot shows that, for small $\tilde{\tau}_F$, the corrections to Stefan-Boltzmann are exponentially small, physically representing the exponentially small amplitude for the “smearing” due to flow to stretch all the way around the periodic direction. However the stability of the result then rather abruptly breaks down above $\tilde{\tau}_F \sim 0.12$, and for large $\tilde{\tau}_F$ values the thermal contribution is almost completely lost. If we require that the flow change the determined energy density by at most 1%, then we can constrain the allowed flow depth to be $8\tau_F/\beta^2 \leq 0.12$. On the lattice with N_t lattice points around the temporal direction, that corresponds to $\tau_F/a^2 \leq 0.015N_t^2$ with a the lattice spacing.

B. Electric-Field Correlation Function at Finite Temperature

In Eq. (1.1) we see that the electric field correlator of interest contains Wilson lines forming a Polyakov loop. However in a lowest-order evaluation these are irrelevant, and only derivatives of the gauge-field propagator are involved. The leading-order contribution reads

$$\begin{aligned} \langle E_i^a(x, \tau_F) E_j^b(0, \tau_F) \rangle & = \partial_0^x \partial_0^y \langle B_i^a(x, \tau_F) B_j^b(y, \tau_F) \rangle \\ & \quad + \partial_i^x \partial_j^y \langle B_0^a(x, \tau_F) B_0^b(y, \tau_F) \rangle \Big|_{y=0}. \end{aligned} \quad (3.8)$$

Differentiating and introducing the dimensionless scaled coordinate $\tilde{x}_n = x_n/\beta$ and the ratio of squared coordinate to flow time $\tilde{\xi}_n^2 = \tilde{x}_n^2/\tilde{\tau}_F$, we find

$$\begin{aligned} & \langle E_i^a(x, \tau_F) E_j^b(0, \tau_F) \rangle \\ &= \frac{g^2 \delta^{ab}}{\pi^2} \sum_{n \in \mathbb{Z}} \frac{1}{\tilde{x}_n^4} \left[\frac{\delta_{ij} (\tilde{x}_n^0)^2 + \tilde{x}_i \tilde{x}_j}{\tilde{x}_n^2} ((\tilde{\xi}_n^4 + 2\tilde{\xi}_n^2 + 2)e^{-\tilde{\xi}_n^2} - 2) \right. \\ & \quad \left. + \delta_{ij} (1 - (1 + \tilde{\xi}_n^2)e^{-\tilde{\xi}_n^2}) \right]. \end{aligned} \quad (3.9)$$

In this expression we have allowed the electric fields to be at different spatial coordinates, but the correlator relevant for heavy quark transport involves $\vec{x} = 0$, which we will set from now on. Our result then simplifies to

$$\langle E_i^a(x^0, \tau_F) E_j^b(0, \tau_F) \rangle = \frac{g^2 \delta^{ab}}{\pi^2 \beta^4} \sum_{n \in \mathbb{Z}} \frac{\delta_{ij}}{\tilde{x}_n^4} [(\tilde{\xi}_n^4 + \tilde{\xi}_n^2 + 1)e^{-\tilde{\xi}_n^2} - 1]. \quad (3.10)$$

This is the main result of this section.

To explore this result further, we consider first the limit of small flow time, $\tilde{\tau}_F \rightarrow 0$ or $\tilde{\xi} \rightarrow \infty$. In this limit $(\tilde{\xi}^4 + \tilde{\xi}^2 + 1)e^{-\tilde{\xi}^2} \simeq 0$. The sum can be performed analytically and the result is

$$\langle E_i^a(x, \tau_F) E_j^b(0, \tau_F) \rangle = -\frac{\pi^2 g^2 \delta^{ab} \delta_{ij} \cos(2\pi \tilde{x}^0) + 2}{\beta^4 3 \sin^4(\pi \tilde{x}^0)}. \quad (3.11)$$

The correlation function is negative, as expected; the electric field is odd under the time-reflection operator

$$E \xrightarrow{\Theta} -E, \quad (3.12)$$

and so its correlation function should be negative. Note however that the time-integrated $\langle EE \rangle$ correlator could still be positive due to contact terms when the operators overlap.

We can also explore the opposite limit of large flow time, $\tilde{\tau}_F \gg 1$, which allows us to approximate the sum over n with an integral,

$$\begin{aligned} & \langle E_i^a(x, \tau_F) E_j^b(0, \tau_F) \rangle \\ & \xrightarrow{\tilde{\tau}_F \gg 1} \frac{g^2 \delta^{ab}}{\pi^2 \beta^4} \int_{-\infty}^{\infty} dn \frac{\delta_{ij}}{\tilde{x}_n^4} [(\tilde{\xi}_n^4 + \tilde{\xi}_n^2 + 1)e^{-\tilde{\xi}_n^2} - 1] \\ &= \frac{g^2 \delta^{ab}}{\pi^2} \frac{\delta_{ij}}{\beta^4 \tilde{\tau}_F^{3/2}} \int_{-\infty}^{\infty} du \frac{1}{u^4} [-1 + (1 + u^2 + u^4)e^{-u^2}] \\ &= \frac{g^2 \delta^{ab} \delta_{ij}}{48 \sqrt{2} \pi^{3/2} \tau_F^{3/2} \beta}, \end{aligned} \quad (3.13)$$

which is the same result we would get by considering only the contribution of the zero Matsubara frequency. In contrast to the small $\tilde{\tau}_F$ limit, this result is positive. There is no contradiction with fundamental theorems, because the operator after flow is no longer local, so Θ -odd behavior does not ensure negative correlations. But this indicates that the result at large flow times has been thoroughly contaminated with contact-term type contributions. Once a correlator which is expected to be negative becomes positive due to flow, the character of the correlation function has been fundamentally altered.

The sum in Eq. (3.10) can be evaluated numerically. In Fig. 3, the behavior of the correlator is shown for different values of $\tilde{\tau}_F$. The black curve is the analytic result for zero flow from Eq. (3.10). The blue curve related to a flow time of $\tilde{\tau}_F = 0.001$ is hidden under the zero-flow curve for $x^0/\beta > 0.2$. Figure 3 shows that as we increase the amount of flow, the x^0 range for which the correlator remains almost unchanged gets narrower; for the larger flow times shown, the two never coincide. Therefore the amount of

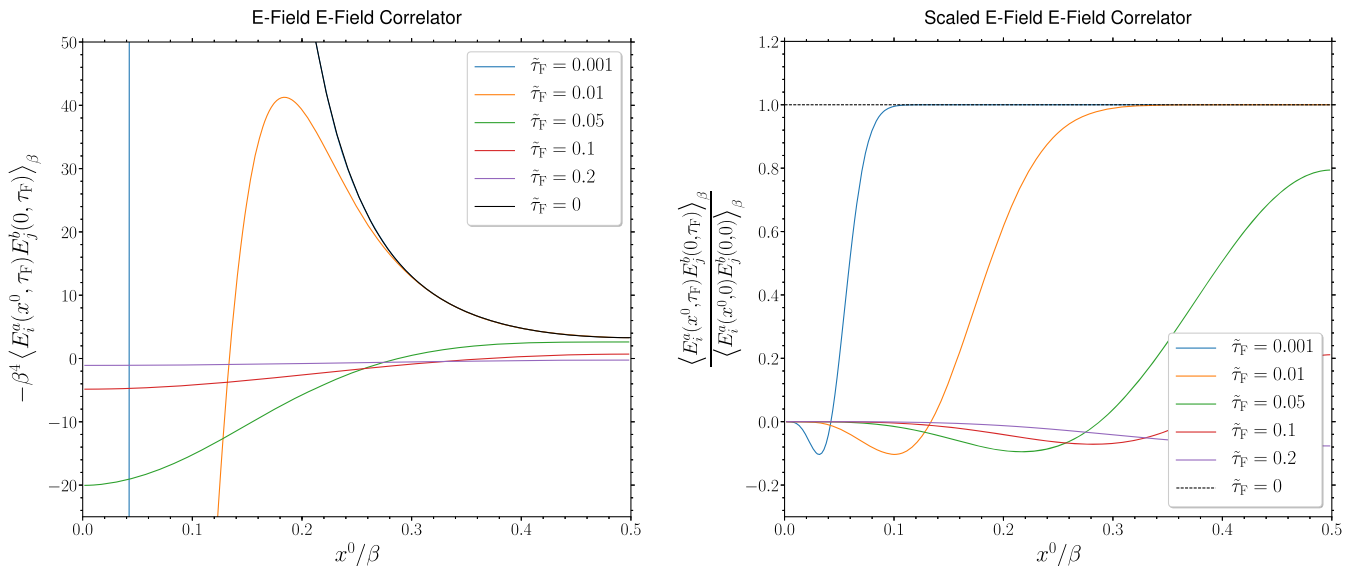


FIG. 3. Left: Plot of the free-theory electric-field electric-field correlation. Right: The same, normalized to the unflowed behavior.

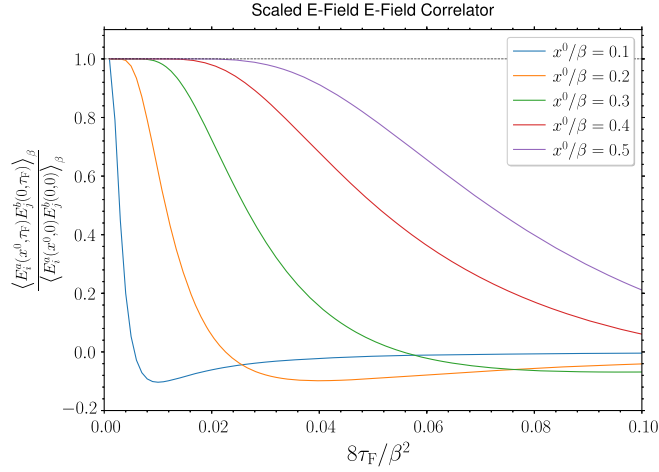


FIG. 4. Plot of the electric-field electric-field correlator normalized to the unflowed behavior at fixed time separations as a function of flow times.

flow which we can “get away with” is x^0 dependent, which should not be too surprising.

It is also instructive to explore the correlator as a function of flow time at fixed separation. Figure 4 shows a plot of this function. The behavior of the function is exactly as expected. For small flow times, the correlator shows a plateau of the unflowed value and the amount of flow which damages the correlator depends on the

$$\begin{aligned} \langle G_{\mu\sigma} G_{\nu\sigma}(x, \tau_F) G_{\alpha\omega} G_{\beta\omega}(0, \tau_F) \rangle &= \frac{d_A g^4}{16\pi^4} C_{\mu\nu\alpha\beta, abcdefgh} \partial_a^x \partial_b^{x'} \partial_c^y \partial_d^{y'} \left\{ \left[\sum_n \frac{\delta_{eg}}{(x-y)_n^2} \left(1 - e^{-\frac{(x-y)_n^2}{8\tau_F}}\right) \right] \left[\sum_m \frac{\delta_{fh}}{(x'-y')_m^2} \left(1 - e^{-\frac{(x'-y')_m^2}{8\tau_F}}\right) \right] \right. \\ &\quad \left. + \left[\sum_n \frac{\delta_{eh}}{(x-y')_n^2} \left(1 - e^{-\frac{(x-y')_n^2}{8\tau_F}}\right) \right] \left[\sum_m \frac{\delta_{fg}}{(x'-y)_m^2} \left(1 - e^{-\frac{(x'-y)_m^2}{8\tau_F}}\right) \right] \right\} \Big|_{x=x', y=y'=0}, \end{aligned} \quad (3.14)$$

where we have introduced the Lorentz structure

$$\begin{aligned} C_{\mu\nu\alpha\beta, abcdefgh} &= (\delta_{\mu a} \delta_{\sigma e} - \delta_{\mu e} \delta_{\sigma a}) (\delta_{\nu b} \delta_{\sigma f} - \delta_{\nu f} \delta_{\sigma b}) \\ &\quad \times (\delta_{\alpha c} \delta_{\omega g} - \delta_{\alpha g} \delta_{\omega c}) (\delta_{\beta d} \delta_{\omega h} - \delta_{\beta h} \delta_{\omega d}). \end{aligned} \quad (3.15)$$

The derivatives can be applied for each sum separately,

$$\begin{aligned} \partial_a^x \partial_c^y \frac{\delta_{eg}}{(x-y)_n^2} \left(1 - e^{-\frac{(x-y)_n^2}{8\tau_F}}\right) \Big|_{y=0} \\ = \frac{4\delta_{eg}}{\pi^2 x_n^4} \left(\delta_{ac} A_n(x, \tau_F) + \frac{x_n a^x x_n c}{x_n^2} B_n(x, \tau_F) \right) \end{aligned} \quad (3.16)$$

with the dimensionless scalar functions defined as

$$A_n(x, \tau_F) = \frac{1}{2} (1 - (1 + \tilde{\xi}_n^2) e^{-\tilde{\xi}_n^2}), \quad (3.17)$$

$$B_n(x, \tau_F) = -2 + (2 + 2\tilde{\xi}_n^2 + \tilde{\xi}_n^4) e^{-\tilde{\xi}_n^2}. \quad (3.18)$$

TABLE I. List of the flow times needed to change the $\langle EE \rangle$ correlator by 1% relative to the zero-flow value, for different x^0 separations.

$\frac{x^0}{\beta}$	$\frac{8\tau_F}{\beta^2}$
0.1	0.0011
0.2	0.0044
0.3	0.0099
0.4	0.0180
0.5	0.0274

separation. If we use more flow, the correlator changes sign. For enough flow it becomes small as all fluctuations are damped away.

In Table I we show the maximum amount of flow before the correlator changes by 1% as a function of x^0 . We believe that this can be used as a criterion for how much flow one can “get away with” in measuring the EE correlator at a given x^0 value.

C. Stress-Tensor Two-Point Functions

The calculation of the stress-tensor two-point correlator is similar to the electric field correlator, except that each stress tensor contains two field strengths. Since there are two gauge field propagators, there is now a double sum over images. The connected stress-tensor two-point function is

Because at leading order $T_{00} = -T_{ii}$, there are three independent stress-tensor correlators (at vanishing spatial momentum) for which we can apply these formulas,

$$\begin{aligned} \langle T_{00} T_{00} \rangle_{\beta}, \quad \langle T_{0i} T_{0i} \rangle_{\beta}, \\ \left\langle \left(T_{ij} - \frac{1}{3} \delta_{ij} T_{kk} \right) \left(T_{ij} - \frac{1}{3} \delta_{ij} T_{ll} \right) \right\rangle \equiv \langle T_{ij}^u T_{ij}^u \rangle, \end{aligned} \quad (3.19)$$

which evaluate to

$$\begin{aligned} \langle T_{00}(x, \tau_F) T_{00}(0, \tau_F) \rangle \\ = \frac{d_A}{\pi^4} \sum_n \sum_m \left[12 \frac{A_n A_m}{x_n^4 x_m^4} + 3 \frac{(A_n B_m + A_m B_n)}{x_n^4 x_m^4} \right. \\ \left. + \left((x_n \cdot x_m)^2 + \frac{1}{2} x_n^2 x_m^2 - 4 \vec{x}^2 x_{n,0} x_{m,0} \right) \frac{B_n B_m}{x_n^6 x_m^6} \right], \end{aligned} \quad (3.20)$$

$$\begin{aligned}
& \langle T_{0i}(x, \tau_F) T_{0i}(0, \tau_F) \rangle \\
&= \frac{d_A}{\pi^4} \sum_n \sum_m \left[24 \frac{A_n A_m}{x_n^4 x_m^4} + 6 \frac{(A_n B_m + A_m B_n)}{x_n^4 x_m^4} \right. \\
&\quad \left. + ((x_n \cdot x_m)^2 + 4x_{n,0}^2 \bar{x}^2 - x_{n,0}^2 x_{m,0}^2 + \bar{x}^4) \frac{B_n B_m}{x_n^6 x_m^6} \right], \tag{3.21}
\end{aligned}$$

$$\begin{aligned}
& \langle T_{ij}^{\text{tr}}(x, \tau_F) T_{ij}^{\text{tr}}(0, \tau_F) \rangle \\
&= \frac{d_A}{\pi^4} \sum_n \sum_m \left[80 \frac{A_n A_m}{x_n^4 x_m^4} + 20 \frac{(A_n B_m + A_m B_n)}{x_n^4 x_m^4} \right. \\
&\quad + \left(10(x_n \cdot x_m)^2 - \frac{52}{3}(x_n \cdot x_m) \bar{x}^2 \right. \\
&\quad \left. + \frac{10}{3}(x_n^2 + x_m^2) \bar{x}^2 + \frac{2}{3} \bar{x}^4 \right) \frac{B_n B_m}{x_n^6 x_m^6} \right]. \tag{3.22}
\end{aligned}$$

These are the main analytic results of this section.

We are interested in the $\vec{p} = 0$ channel and thus need to integrate over $\int d^3x$. At this point we resort to a numerical evaluation. In Fig. 5 the results for the energy-density-energy-density component $\langle T_{00} T_{00} \rangle$ are shown. Energy conservation implies that for vanishing flow time the correlator should be a flat line at a value set by the heat capacity, which in the free theory is $\frac{4\pi^2 d_A}{15\beta^3}$. Such consequences of stress conservation hold up to exponentially small corrections so long as $\tilde{\xi}^2 \gg 1$. However, for larger flow extents, operators effectively overlap, and contact terms contaminate consequences of stress conservation. Therefore, when the flow depth approaches the squared

separation, the constancy of the correlator will be lost. This is indeed what we observe. For large values of flow time $\tilde{\tau}_F \gg 1$, the correlator becomes flat again, as it is dominated by the time-independent zero Matsubara frequency contribution.

The momentum-momentum component $\langle T_{0i} T_{0i} \rangle$ is related to momentum fluctuations in the medium. Without flow, it should be constant and negative, with value set by the enthalpy density times temperature, $\frac{4\pi^2 d_A}{15\beta^3}$. The behavior under flow is shown in Fig. 6. The flow time dependence is similar to that for the $\langle T_{00} T_{00} \rangle$ correlator, for the same physical reasons.

The stress-stress component $\langle (T_{ij} - \frac{1}{3} \delta_{ij} T_{kk}) \times (T_{ij} - \frac{1}{3} \delta_{ij} T_{kk}) \rangle$ is physically interesting because its continuation to a spectral function determines the shear viscosity [34–37]. Because it is not constrained by conservation laws, no short-distance cancellations occur and it shows strong short-distance divergent behavior; the unflowed behavior is dominated by the vacuum contribution which diverges at the origin. If we use gradient flow, the correlator is finite at the origin and for intermediate flow times $0.01 < \tilde{\tau}_F < 0.1$ we find a nontrivial behavior. The numerical results are presented in Fig. 7. For large flow times the zero Matsubara frequency again dominates the correlator, which is nearly x^0 independent.

The main result of this numerical evaluation is that if we are using flow to suppress fluctuations in our correlators, then the $\langle T_{00} T_{00} \rangle$ and $\langle T_{0i} T_{0i} \rangle$ correlators are best evaluated at $x^0 = \beta/2$ and with at most $8\tau_F/\beta^2 < 0.027$. For $\langle T_{ij} T_{ij} \rangle$ one should use the same τ_F values as for the electric field correlator with the same x^0 value.

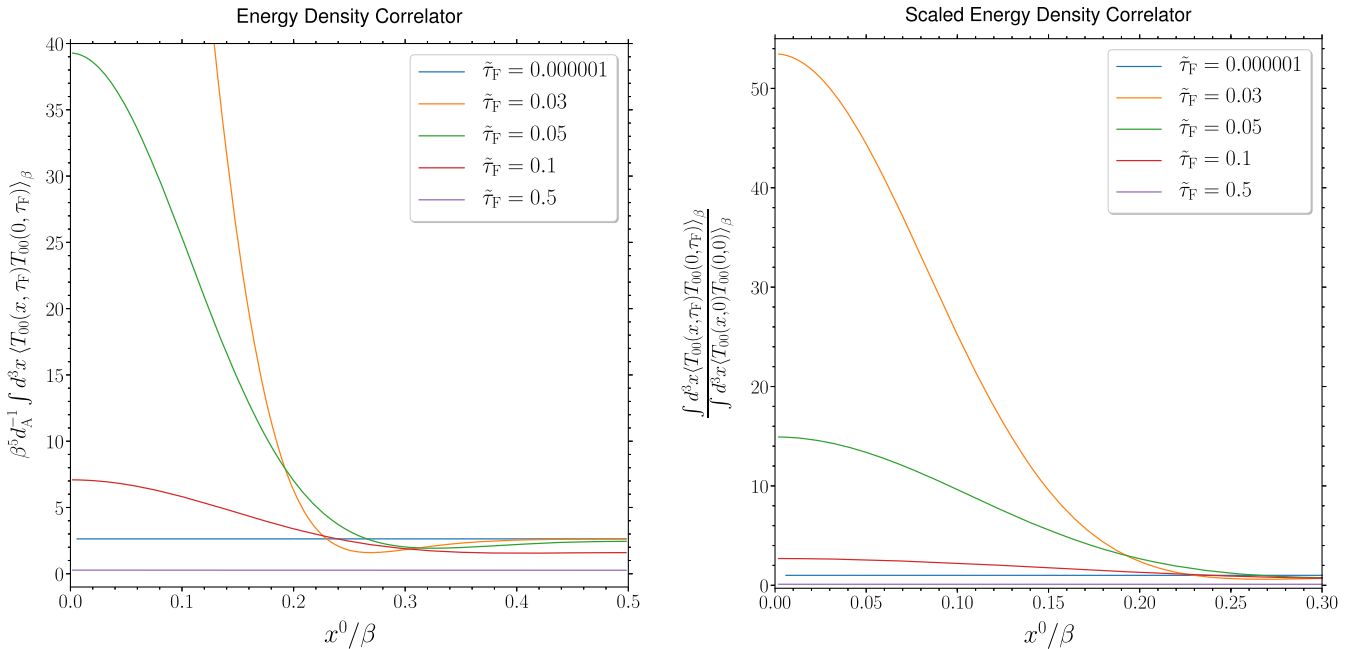


FIG. 5. Plot of the $\langle T_{00} T_{00} \rangle$ correlator at zero spatial momentum as a function of temporal separation, for selected values of flow time.

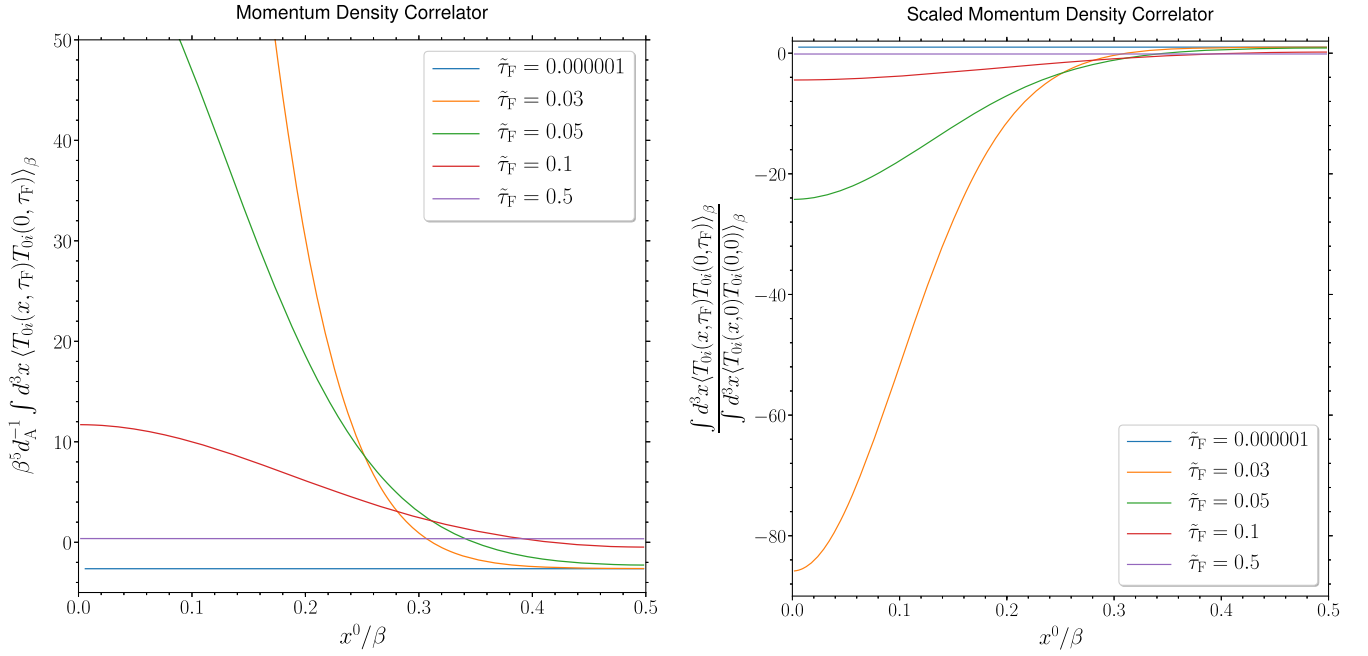


FIG. 6. Momentum density correlator as a function of temporal separation at selected flow depths.

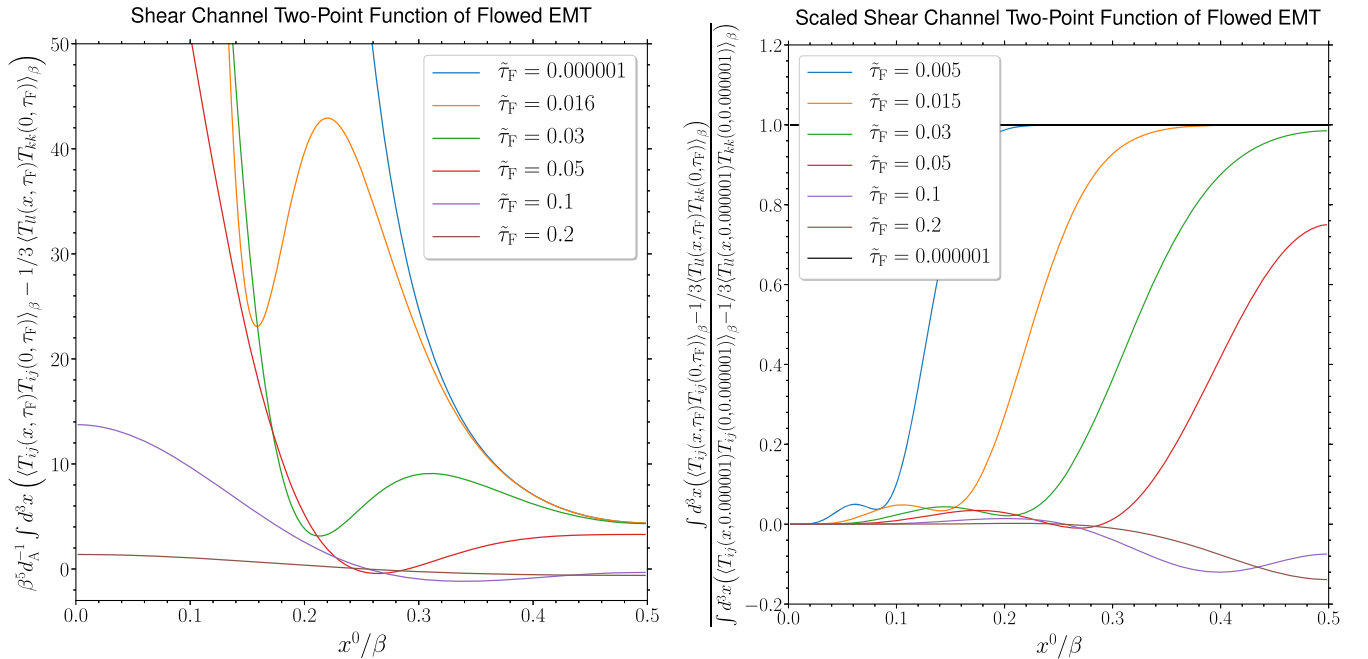


FIG. 7. Left: Plot of the shear channel two-point function of the energy-momentum tensor as a function of temporal separation. Right: The same but normalized to the unflowed result.

IV. DISCUSSION AND CONCLUSIONS

Gradient flow successfully reduces short-distance fluctuations, which is a boon for reducing statistical fluctuations in the lattice determination of local operator correlation functions. Therefore there is interest in applying it to lattice measurements of correlation functions. Here we

made a first exploration of how reliable this approach may be at finite temperature, for the evaluation of the energy density T_{00} and of electric field and stress-tensor two-point functions. At lowest order in perturbation theory, we found that the energy density of the thermal bath is obtained reliably provided that the flow depth obeys $\tau_F < 0.015\beta^2$

(or $\tau_F/a^2 = 0.015N_t^2$ on the lattice), whereas a two-point function of field strengths or stress tensors separated by a distance x^0 is reproduced reliably for $\tau_F < 0.014(x^0)^2$ [or $\tau_F/a^2 = 0.014(\Delta N_t)^2$ on the lattice, where ΔN_t is the minimum number of lattice units of separation between the two operators to be evaluated]. Exceeding this amount of flow causes contact-term contamination in the correlator, either between operators or between an operator and its periodic images. However, below this amount of flow, the effect of flow on the correlation function due to these effects is exponentially small, and consequences of symmetries such as stress-tensor conservation are preserved up to exponential corrections.

It would be valuable to extend this study to the loop level, to see how operator renormalization, the Wilson line appearing in the definition of the electric field two-point function, and other interaction effects enter, and to check whether these effects modify our conclusions.

ACKNOWLEDGMENTS

We thank the Technische Universität Darmstadt and its Institut für Kernphysik, where this work was conducted. This work was supported by the Deutsche Forschungsgemeinschaft (DFG) through the Coordinated Research Center (CRC)-TR 211 “Strong-interaction matter under extreme conditions.”

-
- [1] R. Narayanan and H. Neuberger, Infinite N phase transitions in continuum Wilson loop operators, *J. High Energy Phys.* **03** (2006) 064.
- [2] M. Lüscher, Trivializing maps, the Wilson flow and the HMC algorithm, *Commun. Math. Phys.* **293**, 899 (2010).
- [3] M. Lüscher, Properties and uses of the Wilson flow in lattice QCD, *J. High Energy Phys.* **08** (2010) 071; Erratum, **03** (2014) 92.
- [4] M. Lüscher, Topology, the Wilson flow and the HMC algorithm, *Proc. Sci., LATTICE2010* (2010) 015.
- [5] M. Lüscher and P. Weisz, Perturbative analysis of the gradient flow in non-abelian gauge theories, *J. High Energy Phys.* **02** (2011) 051.
- [6] H. Suzuki, Energy-momentum tensor from the Yang-Mills gradient flow, *Prog. Theor. Exp. Phys.* **2013**, 083B03 (2013); **2015**, 079201(E) (2015).
- [7] C. Monahan and K. Orginos, Finite volume renormalization scheme for fermionic operators, *Proc. Sci., LATTICE2013* (2014) 443.
- [8] C. Monahan and K. Orginos, Locally-smearing operator product expansions, *Proc. Sci., LATTICE2014* (2014) 330.
- [9] M. Lüscher, Future applications of the Yang-Mills gradient flow in lattice QCD, *Proc. Sci., LATTICE2013* (2014) 016.
- [10] K. Hieda, H. Makino, and H. Suzuki, Proof of the renormalizability of the gradient flow, *Nucl. Phys.* **B918**, 23 (2017).
- [11] H. Suzuki, Energy-momentum tensor on the lattice: Recent developments, *Proc. Sci., LATTICE2016* (2017) 002.
- [12] M. G. Prez, A. Gonzalez-Arroyo, L. Keegan, and M. Okawa, The $SU(\infty)$ twisted gradient flow running coupling, *J. High Energy Phys.* **01** (2015) 038.
- [13] R. V. Harlander and T. Neumann, The perturbative QCD gradient flow to three loops, *J. High Energy Phys.* **06** (2016) 161.
- [14] E. Berkowitz, M. I. Buchoff, and E. Rinaldi, Lattice QCD input for axion cosmology, *Phys. Rev. D* **92**, 034507 (2015).
- [15] S. Borsanyi, M. Dierigl, Z. Fodor, S. D. Katz, S. W. Mages, D. Nogradi, J. Redondo, A. Ringwald, and K. K. Szabo, Axion cosmology, lattice QCD and the dilute instanton gas, *Phys. Lett. B* **752**, 175 (2016).
- [16] P. Petreczky, H.-P. Schadler, and S. Sharma, The topological susceptibility in finite temperature QCD and axion cosmology, *Phys. Lett. B* **762**, 498 (2016).
- [17] Y. Taniguchi, K. Kanaya, H. Suzuki, and T. Umeda, Topological susceptibility in finite temperature (2 + 1)-flavor QCD using gradient flow, *Phys. Rev. D* **95**, 054502 (2017).
- [18] F. Burger, E.-M. Ilgenfritz, M. P. Lombardo, M. Müller-Preussker, and A. Trunin, Topology (and axion’s properties) from lattice QCD with a dynamical charm, *Nucl. Phys. A* **967**, 880 (2017).
- [19] J. Frison, R. Kitano, H. Matsufuru, S. Mori, and N. Yamada, Topological susceptibility at high temperature on the lattice, *J. High Energy Phys.* **09** (2016) 021.
- [20] Sz. Borsanyi *et al.*, Calculation of the axion mass based on high-temperature lattice quantum chromodynamics, *Nature (London)* **539**, 69 (2016).
- [21] B. Berg, Dislocations and topological background in the lattice $O(3)$ σ model, *Phys. Lett.* **104B**, 475 (1981).
- [22] M. Asakawa, T. Hatsuda, E. Itou, M. Kitazawa, and H. Suzuki, Thermodynamics of $SU(3)$ gauge theory from gradient flow on the lattice, *Phys. Rev. D* **90**, 011501 (2014); Erratum **92**, 059902(E) (2015).
- [23] M. Kitazawa, T. Iritani, M. Asakawa, T. Hatsuda, and H. Suzuki, Equation of state for $SU(3)$ gauge theory via the energy-momentum tensor under gradient flow, *Phys. Rev. D* **94**, 114512 (2016).
- [24] R. Lohmayer and H. Neuberger, Continuous smearing of Wilson loops, *Proc. Sci., LATTICE2011* (2011) 249.
- [25] R. Lohmayer and H. Neuberger, Rectangular Wilson loops at large N, *J. High Energy Phys.* **08** (2012) 102.
- [26] P. Petreczky and H. P. Schadler, Renormalization of the Polyakov loop with gradient flow, *Phys. Rev. D* **92**, 094517 (2015).
- [27] M. Okawa and A. Gonzalez-Arroyo, String tension from smearing and Wilson flow methods, *Proc. Sci., LATTICE2014* (2014) 327.

- [28] A. Bazavov, N. Brambilla, H. T. Ding, P. Petreczky, H. P. Schadler, A. Vairo, and J. H. Weber, Polyakov loop in $2 + 1$ flavor QCD from low to high temperatures, *Phys. Rev. D* **93**, 114502 (2016).
- [29] C. Monahan and K. Orginos, Quasi parton distributions and the gradient flow, *J. High Energy Phys.* **03** (2017) 116.
- [30] B. A. Berg and D. A. Clarke, Deconfinement, gradient and cooling scales for pure SU(2) lattice gauge theory, *Phys. Rev. D* **95**, 094508 (2017).
- [31] C. Monahan and K. Orginos, Locally smeared operator product expansions in scalar field theory, *Phys. Rev. D* **91**, 074513 (2015).
- [32] S. Caron-Huot, M. Laine, and G. D. Moore, A way to estimate the heavy quark thermalization rate from the lattice, *J. High Energy Phys.* **04** (2009) 053.
- [33] A. Francis, O. Kaczmarek, M. Laine, T. Neuhaus, and H. Ohno, Nonperturbative estimate of the heavy quark momentum diffusion coefficient, *Phys. Rev. D* **92**, 116003 (2015).
- [34] D. N. Zubarev, Non-equilibrium statistical thermodynamics, *Physics Today* **28**, No. 8, 72 (1975).
- [35] F. Karsch and H. W. Wyld, Thermal Green's functions and transport coefficients on the lattice, *Phys. Rev. D* **35**, 2518 (1987).
- [36] H. B. Meyer, A calculation of the shear viscosity in SU(3) gluodynamics, *Phys. Rev. D* **76**, 101701 (2007).
- [37] H. B. Meyer, Transport properties of the quark-gluon plasma: A lattice QCD perspective, *Eur. Phys. J. A* **47**, 86 (2011).
- [38] E. M. Stein and G. L. Weiss, *Introduction to Fourier Analysis on Euclidean Spaces*, Mathematical Series (Princeton University Press, Princeton, NJ, 1971).